water

MDPI

Article

Generation of Homogeneous Slope Units Using a Novel Object-Oriented Multi-Resolution Segmentation Method

Yange Li [1,2], Jianhua He [1], Fang Chen [1], Zheng Han [1,3,*], Weidong Wang [1,2], Guangqi Chen [4] and Jianling Huang [1]

[1] School of Civil Engineering, Central South University, Changsha 410075, China; liyange@csu.edu.cn (Y.L.); 18255110623@163.com (J.H.); csuchenkk@163.com (F.C.); 147745@163.com (W.W.); hjl1201@mail.csu.edu.cn (J.H.)
[2] The Key Laboratory of Engineering Structures of Heavy Haul Railway, Ministry of Education, Changsha 410075, China
[3] Hunan Provincial Key Laboratory for Disaster Prevention and Mitigation of Rail Transit Engineering Structure, Changsha 410075, China
[4] Department of Civil Engineering, Kyushu University, Fukuoka 819-0395, Japan; chen@artsci.kyushu-u.ac.jp
* Correspondence: zheng_han@csu.edu.cn; Tel.: +86-188-7416-3071

Abstract: The generation of map units is a fundamental step for an appropriate assessment of landslide susceptibility. Recent studies have indicated that the terrain relief-based slope units perform better in homogeneity compared with the grid units. However, it is difficult at present to generate high-precision and high-matching slope units by traditional methods. The problem commonly concentrates in the plain areas without obvious terrain reliefs and the junction of sudden changes in terrain. In this paper, we propose a novel object-oriented segmentation method for generating homogeneous slope units. Herein, the multi-resolution segmentation algorithm in the image processing field is introduced, enabling the integration of terrain boundary conditions and image segmentation conditions in slope units. In order to illustrate the performances of the proposed method, Kitakyushu region in Japan is selected as a case study. The results show that the proposed method generates satisfactory slope units that satisfactorily reproduce the actual terrain relief, with the best within-unit and between-unit homogeneities compared with the previous methods, in particular at the plain areas. We also verify the effectiveness of the presented method through the sensitivity analysis using different resolutions of digital elevation models (DEMs) data of the region. It is reported that the presented approach is notably advanced in the requirements of the quality of DEM data, as the presented approach is less sensitive to DEM spatial resolution compared with other available methods.

Keywords: slope unit; object-oriented method; multi-resolution segmentation; DEM spatial resolution; Kitakyushu region

Citation: Li, Y.; He, J.; Chen, F.; Han, Z.; Wang, W.; Chen, G.; Huang, J. Generation of Homogeneous Slope Units Using a Novel Object-Oriented Multi-Resolution Segmentation Method. *Water* **2021**, *13*, 3422. https://doi.org/10.3390/w13233422

Academic Editor: Monica Papini

Received: 1 November 2021
Accepted: 30 November 2021
Published: 3 December 2021

1. Introduction

Recent studies have indicated that landslides are one of the most destructive geological disasters worldwide, causing tremendous property losses and serious fatalities [1]. In order to mitigate landslide hazard, previous studies are devoted to landslide susceptibility analysis. For better analyzing the landslide susceptibility, the selection and generation of map units are the essential preparations [2–5]. These map units aim to segment the entire landslides region into multiple homogeneous units as the minimum calculation units, whose size, shape, and boundary should be consistent with the actual terrain. Therefore, the segmentation effect of map units directly influences the precision of the landslide sensitivity assessment.

To date, the commonly used map units in geography can be briefly categorized into five major types, i.e., grid unit, terrain units, unique-condition units, slope units, and topographic units [6]. Terrain units have long been accepted by previous studies. As the

basis of land system classification, these kinds of units have been applied in many aspects of land resources investigation [7,8], including landslide susceptibility analysis (e.g., [9–11]). Topographic units are defined at the intersection of the contour line and (perpendicular to contour line) flow pipe boundary, reflecting the physical relationship between terrain surface and shallow surface hydrological conditions. It has been applied in predicting surface water saturation state and landslide under terrain control, such as soil sliding and debris flow [12,13]. The grid unit is a regular square with a predetermined size, which is conducive to the analysis of terrain features [14,15]. However, its regularity leads to some losses of the connection with geology, landform, or other landform information. Among the abovementioned units, slope unit has been proved as a better solution that well reflects the terrain and geomorphic characteristics of a large-scale area.

Slope units are portions of the land surface, defined by the general requirement of maximizing homogeneity within a single unit and heterogeneity between different units [16]. The role of the slope unit has received attention across several disciplines in recent years, in particular landslide susceptibility analysis [17–21]. Currently, slope units' formal characterization and practical delineation have been carried out in different ways. Studies have proposed various methods for an automatic generation of slope units based on digital elevation models (DEM). The established methods can be classified into three major categories, including hydrological-based methods, curvature-based methods, and region growth-based methods.

The traditional hydrological-based method aims at extracting slope units from the catchment area and anti-catchment area by hydrological analysis [22,23]. The function of generating slope units using this method has been integrated into the Spatial Analysis Tools—Hydrology toolbox in the ArcGIS environment. However, in the extraction process, the elevation of the area must be reversed forcibly, breaking the law of the formation of a regional water system. Therefore, this treatment often results in some unexpected interferences in the segmentation result. For instance, there will be many small broken surfaces and illogical long strips, leading to a failure of the correspondence between the boundary of units and the actual terrain. In this sense, it requires a lot of manual modification to minimize these unexpected interferences.

Compared with the hydrological-based method, the curvature-based method uses curvature data interpreted from the digital elevation model (DEM), and extracts the catchment area according to similar steps to generate the segmentation of slope units [24]. This method performs better in minimizing the interferences in the segmentation result, particularly at the area with obvious terrain change, where the method is able to generate more uniform units and improve the precision of slope unit partition [25]. However, the curvature-based method is highly sensitive to the resolution of DEM data. It often generates over-tiny slope units with high-resolution DEM data. The large amount of over-tiny slope units requires time-consuming calculations and reduces the heterogeneity between units.

The region growth-based method reproduces the area by iteratively merging adjacent regions with similar terrain features until a certain condition index is satisfied. Remarkable studies can be referred to [26–28]. In many previous studies, the layer data (elevation, curvature, slope, etc.) extracted from the digital terrain model (DEM) are regarded as image data, and the image segmentation algorithm is applied to depict relatively homogeneous slope units. The region growth and classification methods can be also further combined, as carried out by many previous studies [27,29], for the purpose of automatic terrain classification. This method has been proved to be feasible and superior compared with the others [30]. Different studies proposed varied classification criteria and input parameters according to the characteristics of landslide area. As a result, they need to be tailored according to the specific model in use.

Based on the image segmentation algorithm, this paper proposes an object-oriented terrain partition method of slope unit. Starting from the spectral uniformity and spatial correlation of image data, the method combines image segmentation criteria with terrain-limited boundaries such as aspect and drainage area, establishes a specific segmentation

data set and automatic segmentation program, and constructs an automatic slope unit segmentation method based on an image segmentation algorithm. We selected Kitakyushu City as the research area to verify the effectiveness of the method.

2. Automatic Delineation of Slope Units

In this paper, we aim to propose an effective and accurate method of slope unit segmentation by integrating digital terrain into an image segmentation analysis framework. In view of the complexity of surface feature information in a high-resolution image, multiresolution segmentation is introduced to overcome the limitation of traditional methods as mentioned above. At the same time, considering the slope aspect, water system, catchment area, and other factors, the rule sets and automatic segmentation program for image segmentation are established to generate the appropriate slope unit. An evaluation function, which is defined by within-unit homogeneity and inter-unit heterogeneity, is proposed to verify the effectiveness of the proposed segmentation method. The framework of our proposed method is illustrated in Figure 1.

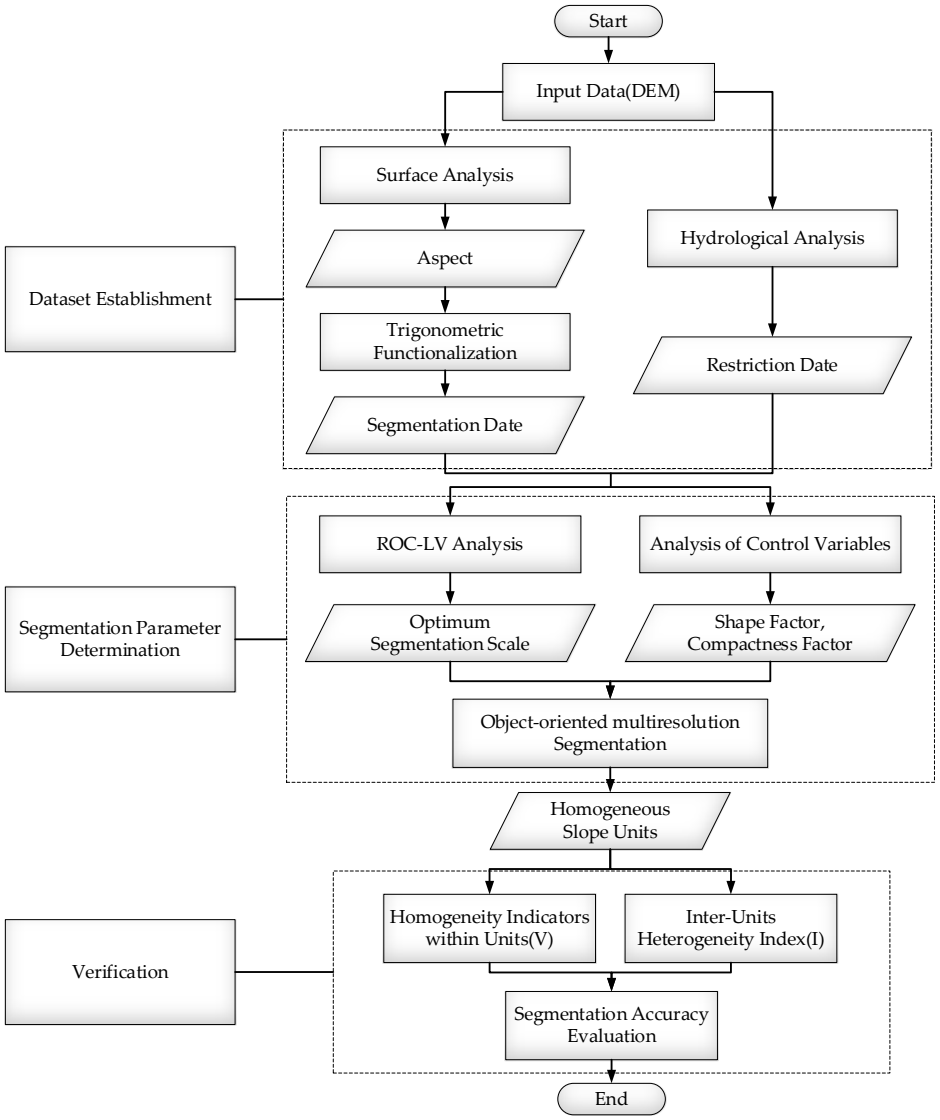

Figure 1. Flowchart for the proposed approach.

2.1. Dataset Establishment

As shown in Figure 1, the first step is to create the multiresolution segmented dataset, including the segmented dataset and the restricted dataset.

2.1.1. The Segmented Dataset

Generally, to obtain a high-precision segmentation result, the terrain factors, e.g., slope, aspect, elevation, curvature, should be directly imported as the segmentation data [31].

Terrain factors are mostly calculated from DEM data. However, the calculation results are often discrepant due to different resolutions of DEM data [32,33]. A previous study [34] indicates that with the increase in the DEM resolution, the mean plane curvature and the average slope gradient increase exponentially and linearly, but the slope aspect remains unchanged. Meanwhile, the high resolution of curvature data leads to the fragmentation of the extraction unit and the complexity of calculation process. When different resolution data are used to extract these terrain factors, the results of slope curvature and slope gradient change significantly compared with the slope aspect [35]. Therefore, the slope aspect is selected as the segmented dataset for slope unit segmentation. This step aims to correct the defect of the existing segmentation method affected by the original data and alleviate the computational burden.

The slope aspect is calculated from the DEM data in the ArcGIS environment. The definition of the slope aspect is shown in Figure 2a, where slope aspect α is defined by the angle between the standard projection of the tangent plane of a point on the surface and the northward direction of the location. It is the maximum change direction describing the elevation change in DEM data. As shown in Figure 2b, the calculated slope aspect α is the azimuth value ranging from 0 to 360 degrees, with the true north direction of 0 degrees. Instead of the slope aspect α, herein we use the trigonometric function to convert slope aspect α into $sin\alpha$ and $cos\alpha$ in X- and Y-direction. This treatment aims to avoid the illogical great aspect difference due to its cyclicity, i.e., the aspects of 1 and 359 degree both denote the directions close to the true north, but aspect difference is illogically as great as 358 degrees (as shown in Figure 2b). This problem can be well addressed using the above trigonometric function.

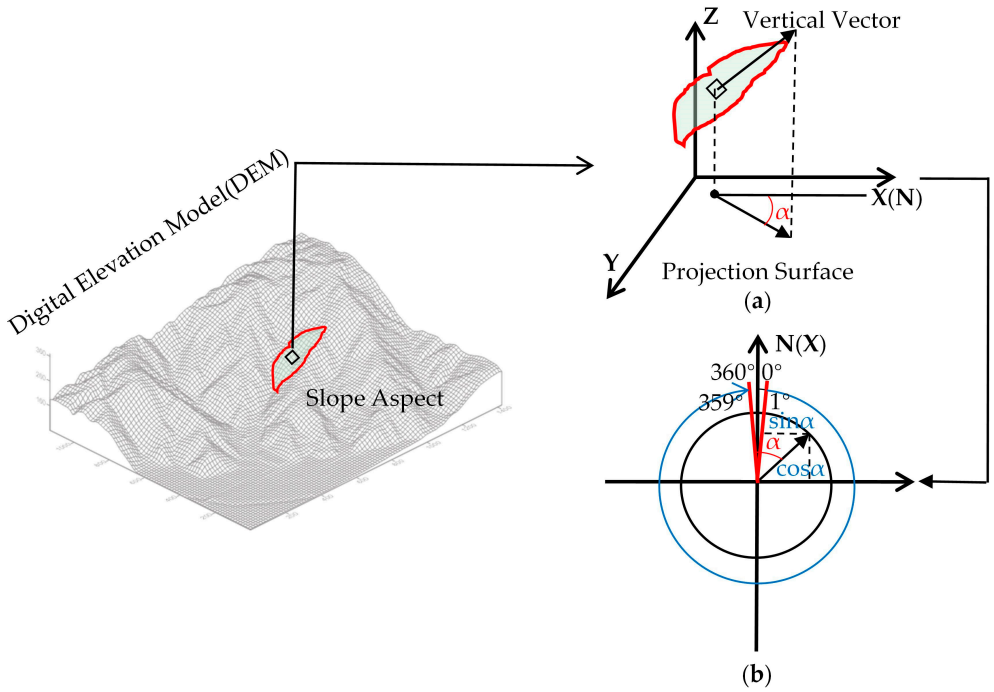

Figure 2. Schematic definition of aspect. (**a**) The definition of slope aspect; (**b**) the calculated slope aspect is the azimuth value ranging from 0 to 360 degrees, with the true north direction of 0 degrees.

2.1.2. The Restricted Dataset

Besides the incised slopes, a catchment usually contains approximately plain terrains without obvious reliefs, such as wide valleys and alluvial fans. Ideally, these plain terrains should not be segmented by the units. However, the conventional methods fail to distinguish the horizontal surface from the inclined surface, because they are mixed in DEM data. As a result, one horizontal slope unit may contain both the inclined surface and the horizontal surface, resulting in obvious errors. To address this problem, terrain boundary information should be integrated into the multiresolution segmentation. Therefore, prior to image segmentation, rational terrain boundary conditions are necessary to improve segmentation quality and efficiency.

It has been widely accepted that the boundary between the positive and negative watersheds extracted by the traditional hydrological method are the ridge lines and valley lines, respectively [25]. A commonly used method, e.g., Zhou et al. [22], is reversing the DEM to obtain the catchment area. However, the divided valleys in the inverted DEM data are forced to terminate when encountering rivers. The hydrological analysis of the valleys can easily create a large area of mostly flat land, which seriously changes the actual surface characteristics. Thus, a large number of illogical long units appear in the formation of catchment areas, whose boundaries do not match the actual topographic lines [36]. However, the boundary of the positive catchment area corresponding to the ridgeline is consistent with the actual topography. Hence, we add the border of the catchment area (ridgeline) as a topographic restriction in the image segmentation method to improve the accuracy of the slope unit segmentation.

According to the technique of catchment extraction in the traditional hydrological method, the positive catchment area is obtained based on the ArcGIS platform. The threshold of the catchment area is a critical parameter for extracting the positive catchment area because the generated digital river network is quite sensitive to this threshold. A greater value of this threshold will commonly result in a sparse river network. Otherwise, an over-dense river network will be generated. The reasonable watershed area value refers to the watershed area value when the extracted river network matches the river network on the topographic map [37]. Therefore, in this paper, based on the river network data, the river system is extracted by referring to the matching degree between the actual data and DEM, to determine the reasonable watershed area threshold. An appropriate threshold of confluence area can ensure the accuracy of the confluence boundary.

2.2. Object-Oriented Multiresolution Segmentation Method

2.2.1. Determination of Segmentation Parameters

Image segmentation is a technology that divides an image into several specific regions with unique properties [38–40], like the principle of slope unit segmentation. In this paper, the multiresolution segmentation algorithm of image segmentation is introduced into the slope unit segmentation, and the quality of segmentation is ensured by terrain boundary conditions and image segmentation standards.

The multiresolution segmentation technique is based on the minimum criterion of heterogeneity [41]. After setting the appropriate segmentation parameters, starting from a random pixel in the target image, the heterogeneity after merging with adjacent pixels is calculated and compared with the segmentation scale. If the heterogeneity condition is satisfied, the cell can continue to be merged. Otherwise, the segmentation process ends. Accordingly, important segmentation parameters in the multiresolution segmentation algorithm include segmentation scale and heterogeneity factor.

The primary concern of extracting slope units based on multi-resolution segmentation technique is the segmentation scale of the image objects. The segmentation scale directly determines the size of the segmented object: the larger the scale is, the larger the object is. Otherwise, this object just shatters. For slope unit segmentation, it is necessary to ensure that the image object size is consistent with the target slope size and contour. The segmentation scale currently is the optimal segmentation scale. Only by setting

reasonable segmentation parameters can we obtain results close to the actual landslide scale. Otherwise, the phenomenon of "under-segmentation" or "insufficient segmentation" may occur in the segmentation result [42,43].

The previous studies have widely used repeated experiments and visual observation methods to determine the optimal segmentation scale, which has high requirements for researchers and is difficult to popularize and apply. In this paper, the local variance (*LV*) curve [44–46] is used to determine the optimal parameters for fast and effective application. The method calculates the average value of the local variance in the window through the $n \times n$ pixel-moving window and generates a local variance value LV_a, and the calculation formula is as follows:

$$LV_a = \frac{\sum_{i=1}^{M-1} \sum_{j=1}^{N-1} LV(i,j)}{MN}, \quad (1)$$

where M and N represent the size of the original image row and column; i and j are the number of local window rows and columns; $LV(i,j)$ represents the variance of the local image gray value within the window size and the calculation formula is:

$$LV(i,j) = \sqrt{\frac{\sum_{i=0}^{n} \sum_{j=0}^{n} [f(i,j) - f]^2}{n^2}} \quad (2)$$

where n represents the window size; $f(i,j)$ represents the gray level of the ith row jth column pixels in the local window; and f is the local window pixel gray-scale mean.

The window size is determined by the size of the segmentation scale. If the segmentation scale is excessively small, the window size becomes smaller. Moreover, the higher the homogeneity in the image object is, the lower the heterogeneity between the image objects is, resulting in a low LV_a. As the segmentation scale gradually approaches the optimal scale, the heterogeneity between image objects increases and LV_a also increases. When the segmentation scale is oversized, LV_a gradually decreases. Therefore, the parameter LV_a can be used as an index to evaluate the quality of image segmentation.

In order to evaluate the dynamic change in LV_a with the size of the segmentation, detailed information of the actual performance of the segmentation effect can be obtained by means of the *ROC-LV* [47] curve (rate of change of *LV*). The *ROC-LV* curve reflects the rate of change of the average local variance as a function of window size, which is the dynamic change between the target layers obtained at different segmentation scales. The segmentation scale corresponding to the peak point of the curve is the closest to the actual size of the object, which is the optimal segmentation scale for multiresolution segmentation.

$$ROC - LV = \left[\frac{L - (L-1)}{L-1} \right] \times 100 \quad (3)$$

The heterogeneity factor consists of spectral heterogeneity and shapes heterogeneity, which directly defines the calculation of heterogeneity and affects the final segmentation result, together with the segmentation scale [48]. The sum of spectral heterogeneity and shape heterogeneity is one. Simultaneously, the shape heterogeneity is determined by the compactness factor and the smoothness factor, and the sum is one. In general, the shape heterogeneity factor and the compactness factor are determined, and the whole heterogeneity parameter is determined. Most of the existing parameter determination methods are empirical value determination and lack a quantitative basis [49,50]. Based on the principle of minimum heterogeneity, the experiment is performed using the control variable method. First, select a segmentation scale randomly, and then adjust the shape factor to find the optimal compactness. The same method is used to determine the shape factor. In addition, we follow the effective experience [51]: the shape index value should be relatively small, and the tightness value is relatively large, accurately defining the shape factor and tightness to ensure the quality of the segmentation.

2.2.2. Object-Oriented Multiresolution Segmentation Algorithm

Due to the change in local vegetation, hillshades by mountains, and complex illumination conditions, the spectral features of slopes may vary in the remote sensing images, creating various challenges in using interchangeable methods for unit extraction. In remote sensing images, the size of typical landslide units is different, making it burdensome to select a single segmentation scale to segment the image effectively. Thus, the multiresolution segmentation method is adopted to improve the segmentation precision by establishing different scales of segmentation and layer-by-layer segmentation.

The multiresolution segmentation method based on remote sensing images can generate image polygons (objects) with arbitrary scale and similar attribute information and take image objects as the basic unit of information extraction to realize classification and information extraction. The multiresolution image segmentation starts from any pixel and uses the bottom-up region-merging method to form objects. Small objects can be merged into large objects through several steps, and the size of each object must be adjusted to ensure that the heterogeneity of merged objects is less than a given threshold [52,53]. The necessary steps are as follows (as illustrated in Figure 3):

1. Data import: The regional DEM data should be imported to generate a slope aspect dataset, which is used as the basic layer for image segmentation. Ridge lines extracted from the forward catchment area can also be obtained using DEM data, and then are considered as the thematic restriction layer.
2. Parameter setting: the *ROC-LV* method is used to determine the optimal segmentation scale, and the optimal shape factor and compactness are determined according to the requirements.
3. Segmentation: Multiresolution image segmentation adopts a bottom-up segmentation method. The first segmentation starts from any pixel in the image, and the initial heterogeneity parameter is calculated. After the first segmentation, the second segmentation is performed based on the new image region. If the heterogeneity parameter f is small compared with the square of the segmentation scale, the segmentation is continued; if the heterogeneity parameter f is small compared with the square of the segmentation scale, the segmentation is continued according to the minimum heterogeneity criterion, and the segmentation ends when all the pixels in the image are divided into different image objects.

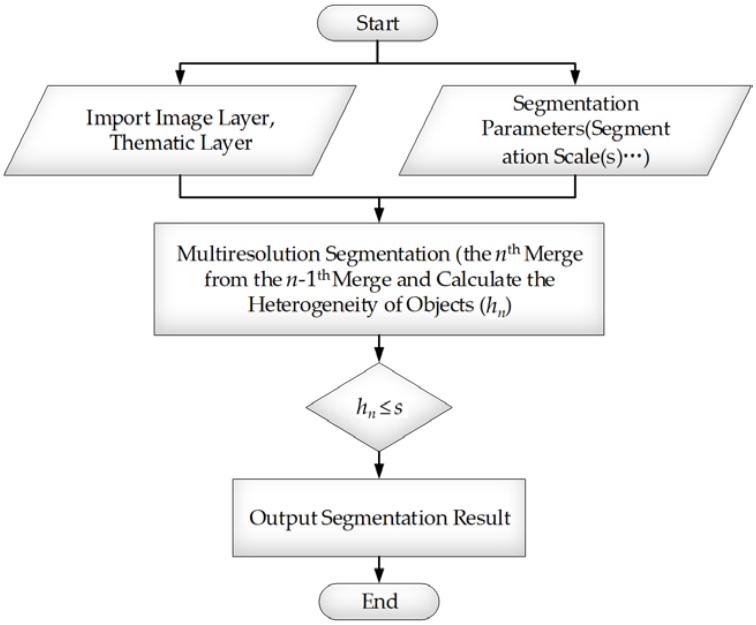

Figure 3. Schematic diagram of multiresolution segmentation algorithm.

2.3. Segmentation Metric of Slope Unit Segmentation Method

To evaluate the terrain partitioning into slope units, we adopt an initial segmentation metric for the evaluation of the quality of segmentation results. In digital image processing, segmentation is the process of dividing an image into several pixel sets, so that the pixels in the same pixel set have some common features. Here, we consider the terrain orientation raster image as the image to be segmented, and assume that the segmentation metric proposed by Espindola et al. [51] is suitable for evaluating terrain segmentation in slope units.

This segmentation metric is based on the principle that in digital image processing, segmentation divides an image into several groups of pixels so that the same group of pixels has certain homogeneity and different groups of pixels have heterogeneity [54]. It combines the local circular variance value (index V) describing the homogeneity of objects with the Moran index (index I) value representing the heterogeneity between objects and constructs a segmentation quality evaluation function $F(V,I)$ to evaluate the quality of DEM data. The above parameters are defined as follows:

$$V = \frac{\sum_n S_n C_n}{\sum_n S_n} \tag{4}$$

$$I = \frac{N \sum_{n,l} \omega_{nl} (\alpha_n - \overline{\alpha})(\alpha_l - \overline{\alpha})}{(\sum_n (\alpha_n - \overline{\alpha})^2)(\sum_{n,l} \omega_{nl})} \tag{5}$$

where N is the total amount of units; n denotes the number of each individual unit; S_n is the surface area of the nth slope unit; C_n is the circular variance of the aspect in the nth slope unit; α_n is the average aspect of the nth slope unit; and $\overline{\alpha}$ is the average aspect of the entire terrain aspect map. Moreover, ω_{nl} is an indicator of spatial proximity; if slope unit n and l are adjacent, it is equal to one, otherwise zero. The local variance V defined in Equation (4) is more critical for large slope units, avoiding the numerical instability caused by small slope units. The lower the value, the higher the homogeneity within the unit. The autocorrelation index I in Equation (5) has a minimum value when there is high heterogeneity between different slope units. The best choice of DEM resolution is the combination of small V and small I. This is determined by the following objective function:

$$F(V, I) = \frac{V_{max} - V}{V_{max} - V_{min}} + \frac{I_{max} - I}{I_{max} - I_{min}} \tag{6}$$

where $V_{\min(max)}$ and $I_{\min(max)}$ are the minimum (maximum) values of the quantities in Equations (4) and (5). The aspect map is displayed in a degree form. It is not possible to calculate the mean and variance straightforwardly and there is a massive difference in value between 0 degrees and 359 degrees, but only a 1-degree difference in azimuth. We know that the mean of degrees is the vector sum of the unit vectors. Therefore, we convert it into radians and make the following definitions:

$$\overline{\alpha} = arctan\left(\frac{\sum_j sin\alpha_j}{\sum_j cos\alpha_j}\right) \tag{7}$$

where the j labels run over all the slope units on the entire terrain map. Analogously, we define for α_i the average aspect inside the ith slope unit, according to Equation (7). The difference $(\alpha_i - \overline{\alpha})$ should also be a vector, as follows.

Then, the numerator of Equation (5) is evaluated by:

$$(\alpha_i - \overline{\alpha}) \cdot (\alpha_j - \overline{\alpha}) = cos\theta_i cos\theta_j + sin\theta_i sin\theta_j \tag{8}$$

where θ_i and θ_j are denoted as following, respectively:

$$\theta_i = arctan\left(\frac{sin\alpha_i - sin\overline{\alpha}}{cos\alpha_i - cos\overline{\alpha}}\right) \tag{9}$$

$$\theta_j = arctan\left(\frac{sin\alpha_j - sin\overline{\alpha}}{cos\alpha_j - cos\overline{\alpha}}\right) \quad (10)$$

The segmentation metric is a measure of the internal homogeneity and external heterogeneity of slope units, which is related to the geometry and shape of slope units. This metric can be used to assess the optimal segmentation of slope units by maximizing function $F(V, I)$. Besides, the remote sensing images commonly used in existing research have multiple spatial resolutions, and the spectral, texture and structural features of data with different spatial resolutions have different degrees of variation. The role of the spatial resolution of data in geological research cannot be ignored [55–57]. Therefore, in order to investigate the sensitivity of the proposed method to the DEM resolution, four groups of results using different DEM resolutions will be compared in the following case study section.

3. Case Study

3.1. Study Area

To verify the proposed method, Kitakyushu in Japan was selected as a study area. The area is located in Fukuoka County, the economic center of Kyushu (as shown in Figure 4). Most of the area is mountainous and has a humid climate, with an average rainfall of approximately 1265 mm per year. From 1989 to 2005, many landslides were recorded due to the impact of earthquakes and heavy rainfalls, causing tremendous fatalities and economic losses. In this paper, we apply the proposed method to generate slope units. The collected DEM data in this area have varying resolutions of 5 m, 10 m, 30 m, and 90 m. The 90 m and 30 m resolution DEM data are available in SRTM1 and SRTM3 data products. The 10 m resolution DEM data are collected from the Geological Information Authority of Japan (GSI), while the 5 m resolution data are from the altitude data set that was produced and made open to public by Japan Geographic Bureau using LIDAR [3]. In order to eliminate the errors caused by different coordinate systems, we transferred all first coordinate systems to GCS_WGS_1984 parallel systems. The results were then compared with the previous hydrological- and curvature-based method to evaluate the correctness and superiority of the proposed method in this paper.

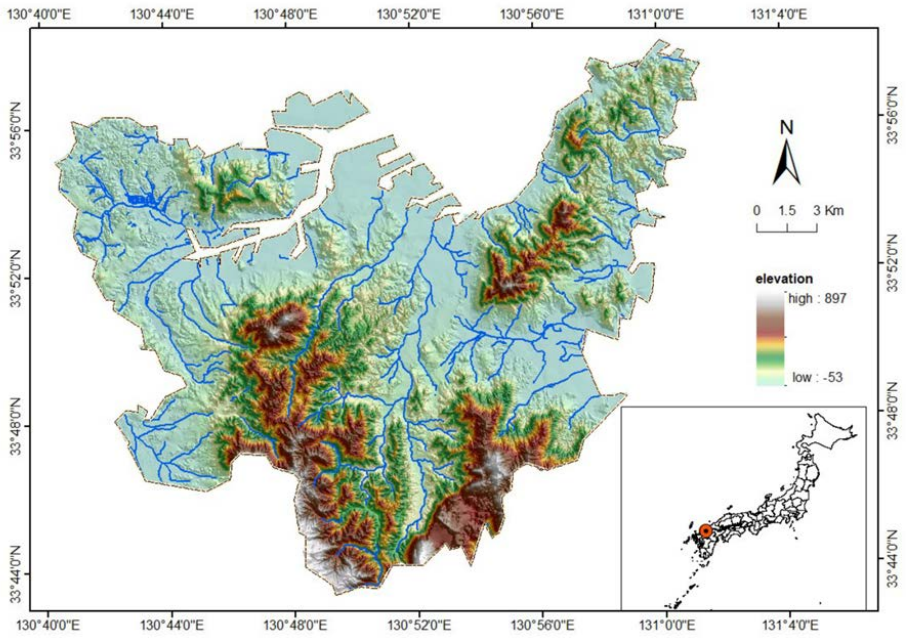

Figure 4. Overview of the study area, Kitakyushu region.

3.2. Results

In the study area, we used the presented novel object-oriented multiresolution segmentation method to generate slope units from four groups of DEM data with different spatial resolution. In the segmentation procedure, the positive catchment area extracted from each DEM data set was used as the terrain constraint. Owing to that segmentation scale, the shape factor and compactness factor determine the size and control the aspect of the slope units; we calculated these parameters using the proposed method as mentioned in Section 2.2. The obtained parameters determined by the four-resolution data are listed in Table 1.

Table 1. Parameters used in object-oriented multiresolution segmentation.

DEM Data Resolution	Shape Factor	Compactness Factor	Optimum Segmentation Scale
90 m	0.15	0.5	8
30 m	0.3	0.5	8
10 m	0.1	0.5	9
5 m	0.1	0.5	8

Figure 5 shows the results of the terrain subdivisions obtained using different modeling parameters. The maps in the right panel show the detailed slope units partitioning. In particular, Figure 5a–d show the overlaying slope units on the hill-shade maps of the example area, with different spatial resolution of DEM data. It is shown that along with the increasing DEM spatial resolution, the generated slope units increase in density and show a corresponding decrease in their average size.

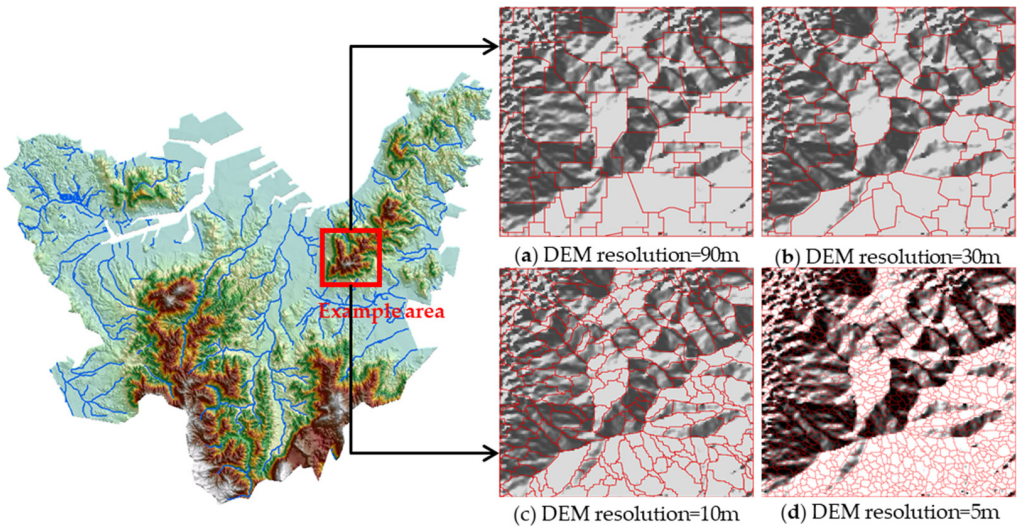

Figure 5. Example of slope unit subdivisions for a portion of the study area. Enlarging the "Example area" to illustrate the segmentation results obtained by the multiresolution segmentation method with different resolution data. Red lines show the boundaries of slope units, while gray areas are hill shade. (**a**) DEM resolution = 90 m; (**b**) DEM resolution = 30 m; (**c**) DEM resolution = 10 m; (**d**) DEM resolution = 5 m.

4. Comparison

To verify the correctness and accuracy of the proposed method, the traditional hydrological-based method and the mean-curvature-based method are used as a comparison. In this section, we choose the best segmentation result of each method using the optimal parameters. The generated slope units using the three methods with different DEM data are shown in Figures 6 and 7.

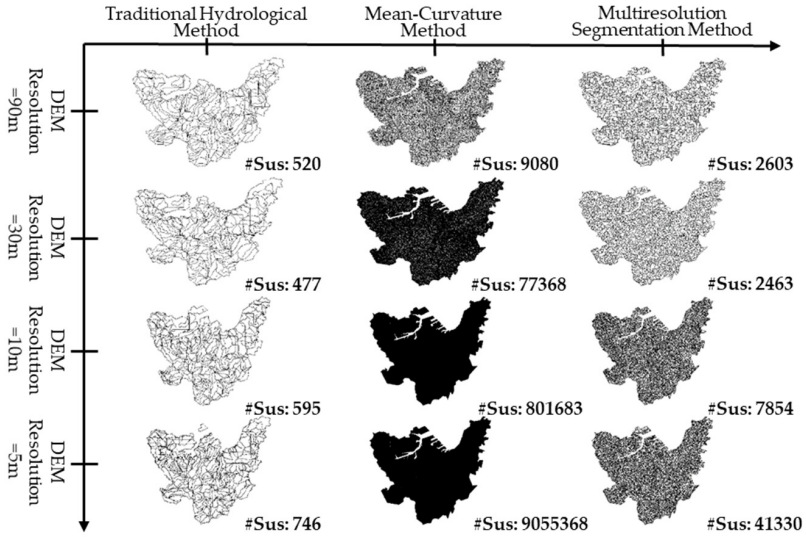

Figure 6. Slope units partitioning obtained from the 5 m, 10 m, 30 m and 90 m resolution DEM data, using three different slope units segmentation methods.

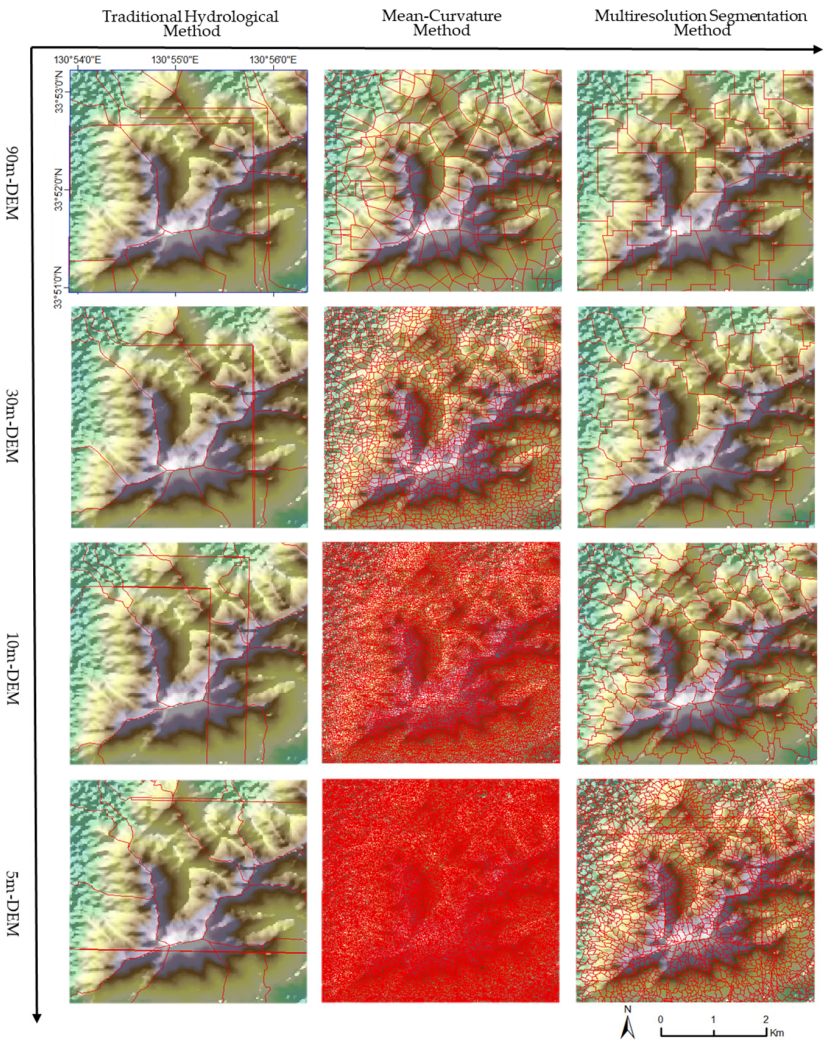

Figure 7. Comparison of the three different slope unit segmentation methods against different DEM resolutions. Details in the selected example area, as marked in Figure 5.

As shown in Figures 6 and 7, in the traditional hydrological-based method, the number of extracted slope units is 520 in total. It is observed that lots of narrow fracture units and parallel boundaries appear, in particular at the plain areas with flat terrain, while in the mountainous areas with terrain reliefs, errors could be observed as the partitioned slope units appears to be inconsistent with the actual terrain lines. These inconsistences seem to be improved with the increase in DEM spatial resolution. However, the partitioned slope units are still over large, failing to represent the terrain reliefs. In this sense, the slope units obtained by the traditional hydrological-based method have a low degree of matching and the segmentation precision is relatively low.

The middle column of the maps in Figure 7 shows the results by the mean-curvature method. Obviously, compared with the traditional hydrological-based method, the partitioned slope units are evenly distributed and uniform in size. However, the extracted units are numerous and over tiny. With the increase in spatial resolution, the number of slope units increases dramatically, extending towards 9,055,368. Although the unit boundaries are majorly consistent with the actual terrain, a high number of over-tiny slope units requires time-consuming calculations, and reduces the heterogeneity between units.

As shown in the right column of the maps in Figure 7, the proposed object-oriented multiresolution segmentation method divides the area into uniformly sized units, but the number of units is less than by the mean-curvature-based method. The increasing DEM spatial resolution also leads to an increasing number of slope units. However, compared to the mean-curvature method, the results are no more sensitive to the DEM resolution. In addition, the proposed multiresolution method generates the slope units well under four different DEM resolutions, without obvious parallel interferences that exist in the results by the traditional hydrological method, and the obtained slope units substantially coincide with the actual terrain.

The quantitative difference between the proposed method and the previous methods can be described by the quality evaluation function $F(V, I)$ introduced in Section 2.3. The results are shown in Figure 8.

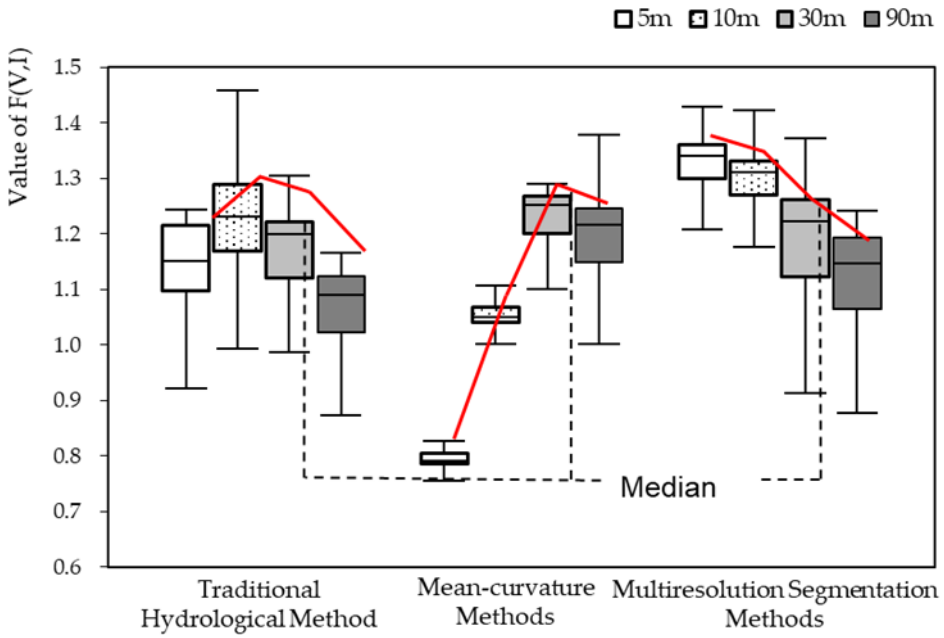

Figure 8. Variation in $F(V, I)$ values against different DEM resolutions by the proposed segmentation method and previous methods.

Figure 8 describes variation in $F(V, I)$ values against different DEM resolutions by the proposed segmentation method and previous methods. As introduced in Section 2.3, $F(V, I)$ is a function for evaluating segmentation qualities. A greater value of $F(V, I)$

indicates a better quality of segmented slope units with homogeneity and heterogeneity. As shown in Figure 8, the proposed multiresolution method performs best because the obtained results have the greatest values of $F(V, I)$ in general, in particular with the DEM resolution of 5 m and 10 m. As to the 30 m and 90 m resolution DEM data, three methods approximate $F(V, I)$, and the mean-curvature method generates the best results; however, it generates many tiny slope units, as shown in Figure 6. As such, the proposed multi-resolution method is a flexible solution for generating slope units with high resolution DEM data, because the $F(V, I)$ increases almost linearly with the DEM solution.

5. Discussion

In this paper, an object-oriented multi-resolution segmentation method is proposed for generating homogeneous slope units. Compared with the traditional pixel-based grid units, the generated high-homogeneous slope unit combines the pixels with similar slope aspect properties into a meaningful geomorphic object. Therefore, this method is object-oriented, and produces results that are verifiable and can easily be converted to GIS data. We ran the proposed segmentation method with corresponding segmentation parameters. The results show that the proposed method can better divide the study area into slope units, with high homogeneity and heterogeneity.

As shown in the calculation of the evaluation function $F(V, I)$, it is noted that for the three methods mentioned, DEM data with higher resolution do not necessarily correspond to the best segmentation results. In our study, the results obtained from DEM data with the 5 m resolution do not show the best performance. For the two conventional segmentation methods, the evaluation function F value is of the inverted "V" type as the resolution decreases. In other words, for the traditional hydrological method, in the range of 90 to 10 m resolution, the $F(V, I)$ value is increased, and the quality of the segmentation unit becomes more advantageous. The segmentation metric $F(V, I)$ reaches a maximum value at 10 m resolution for the optimal segmentation quality. When the data are of a more meticulous 5 m resolution, the F value becomes trifling and slope unit segmentation quality is lowly. For the mean-curvature method, the peak point of the inverted V-curve appears at 30 m spatial resolution. Resolution data above 30 m and below 30 m split out units with lower F values, which have inferior segmentation accuracy.

As a matter of fact, depending on the type of landslides, the scale of the available DEM, the morphological variability of the landscape, and the purpose of the zonation, the detail of the terrain subdivision may vary. Scholars have proved that the resolution of DEM has a significant impact on the slope unit segmentation, but it will not change the logic of the approach or the rationale behind our optimization method. We clarify that the subdivision units generated by the segmentation parameters used in this method are nested, that is, the boundaries of the coarse resolution subdivision encompass the boundaries of the intermediate subdivision and finer subdivision. Schlögel et al. [54] proposed the automatic unit segmentation and landslide sensitivity assessment of R. Slopeunits v1.0 under different DEM resolutions. They believed that if only F-measure was used to select a specific set of modeling parameters, the best set of slope units only had the meaning of "the best slope unit subdivision for a particular goal". Similarly, the $F(V, I)$ metric only considers the homogeneous and heterogeneous features of a single slope unit, but the matching degree with the actual terrain boundary is not fully considered (for example, too large, too irregular, too small). Therefore, we adopted the catchment boundary as the terrain boundary constraint, and maximized the value of evaluation function $F(V, I)$ to achieve the optimization of element segmentation and improve the accuracy,

As for the segmentation result of the multiresolution segmentation method, the split metric F value increases as the data resolution increases. In the four test sets of DEM spatial resolution, no peaks appeared. However, the rate of increase in F value from 5 m resolution to 10 m resolution is small. From the calculation amount, the number of units increases ten times, yet the $F(V, I)$ value only increases by 0.03. Therefore, when using the multiresolution segmentation method, 10 m resolution data are beneficial.

6. Conclusions

The limited use of slope units for landslide sensitivity modeling is due to the unavailability of high-precision, easy-to-use methods for automatic delineation. In order to fill this gap, we propose a new method for the automatic delineation of slope units in complex geographical areas based on the multiresolution segmentation algorithm and catchment terrain constraints. We further proposed and tested the segmentation metric for comparative verification of the method in Kitakyushu, Japan.

Compared with the existing conventional methods, the multiresolution segmentation method limits the boundary of the catchment area as the terrain condition of image segmentation, and relies on image segmentation parameters to realize the segmentation of complex terrain. Different from the homomorphic units, the fine units divided by the traditional hydrological method and the low homogeneity units divided by the mean-curvature method, the multiresolution segmentation method has uniform unit size and regular shape and matches the actual terrain, avoiding complicated manual editing. Moreover, by calculating the value of the segmentation metric $F(V, I)$, the intra-unit homogeneity and inter-unit heterogeneity are more advanced than the two existing methods. Finally, this method has generality and can be popularized. It is more suitable for current landslide research and has substantial research value.

In addition, we propose a procedure to determine the optimal DEM spatial resolution in each slope unit segmentation. The procedure is developed within the framework of the evaluation of slope units. Homogeneous slope units are produced automatically with the traditional hydrological, the mean-curvature and the multiresolution segmentation methods. We use four DEMs with spatial resolutions of 5, 10, 30 and 90 m, and measure the performance of a segmentation metric as a function of different slope unit delineations. The segmentation metric function combines the homogeneity index within the unit and the heterogeneity index between the units. Maximization of the metric function provides the optimal DEM spatial resolution for each partitioning.

We compared the resulting twelve sets of values of the segmentation metric based on an analysis of the statistical significance of the thematic and morphometric variables. According to the calculation results, the spatial resolution of DEM plays a vital role in the accuracy of the slope unit segmentation. We find that the optimal segmentation results do not necessarily appear in DEM data with the highest resolution. Different slope unit segmentation methods have particular optimal DEM spatial resolution. In traditional hydrological methods, DEM data with a resolution of 10 m are the most suitable for segmentation. DEM data with a resolution of 30 m play an essential role in the mean-curvature method. DEM data with a resolution of 10 m have a similar accuracy to those of a 5 m resolution; however, based on the amount of calculation required, 10 m resolution is the most economical and effective segmentation method in the multiresolution slope unit segmentation method for Kitakyushu region. However, for other regions worldwide, whether the 10 m resolution achieves the best result requires more tests. We further emphasize the influence of DEM spatial resolution on the segmentation accuracy of slope units and provide a reference for data selection in the subsequent landslide study.

Author Contributions: Z.H. led the research program. Y.L., J.H. (Jianhua He) and G.C. designed the algorithm. Y.L. and F.C. wrote the manuscript. G.C., W.W. and J.H. (Jianling Huang) reviewed and edited the manuscript. All authors have read and agreed to the published version of the manuscript.

Funding: This study was founded by the National Key R&D Program of China (grant number 2018YFD1100401); the National Natural Science Foundation of China (grant number 52078493); the Natural Science Foundation for Outstanding Youth of Hunan Province (grant number 2021JJ20057); and the Innovation Province Program of Hunan Province (grant number 2020RC3002).

Institutional Review Board Statement: Not applicable.

Informed Consent Statement: Not applicable.

Data Availability Statement: The data used in this study are available on request from the corresponding author.

Conflicts of Interest: The authors declare no conflict of interest.

References

1. Lu, P.; Stumpf, A.; Kerle, N.; Casagli, N. Object-Oriented Change Detection for Landslide Rapid Mapping. *IEEE Geosci. Remote Sens. Lett.* **2011**, *8*, 701–705. [CrossRef]
2. Guzzetti, F.; Reichenbach, P.; Ardizzone, F.; Cardinali, M.; Galli, M. Estimating the quality of landslide susceptibility models. *Geomorphology* **2006**, *81*, 166–184. [CrossRef]
3. Saito, H.; Nakayama, D.; Matsuyama, H. Comparison of landslide susceptibility based on a decision-tree model and actual landslide occurrence: The Akaishi Mountains, Japan. *Geomorphology.* **2009**, *109*, 108–121. [CrossRef]
4. Li, Y.G.; Liu, X.T.; Han, Z.; Dou, J. Spatial proximity-based geographically weighted regression model for landslide susceptibility assessment: A case study of Qingchuan area, China. *Appl. Sci.* **2020**, *10*, 1107. [CrossRef]
5. Wang, W.D.; He, Z.L.; Han, Z.; Li, Y.G.; Dou, J.; Huang, J.L. Mapping the susceptibility to landslides based on the deep belief network: A case study in Sichuan Province, China. *Natural Hazards.* **2020**, *103*, 3239–3261. [CrossRef]
6. Huabin, W.; Gangjun, L.; Weiya, X.; Gonghui, W. GIS-based landslide hazard assessment: An overview. *Prog. Phys. Geogr. Earth Environ.* **2016**, *29*, 548–567. [CrossRef]
7. Lopes, R.P.; Madeira, M.; Arsénio, P. Mapping of Land Units and Land Capability Classification in Portugal. The Case of the Municipality of LourinhÃ. *Finisterra* **2018**, *52*. [CrossRef]
8. Saha, S.; Paul, G.C.; Hembram, T.K. Classification of terrain based on geo-environmental parameters and their relationship with land use/land cover in Bansloi River basin, Eastern India: RS-GIS approach. *Appl. Geomat.* **2019**, *12*, 55–71. [CrossRef]
9. Can, T.; Nefeslioglu, H.A.; Gokceoglu, C.; Sonmez, H.; Duman, T.Y. Susceptibility assessments of shallow earthflows triggered by heavy rainfall at three catchments by logistic regression analyses. *Geomorphology* **2005**, *72*, 250–271. [CrossRef]
10. Li, J.Y.; Wang, W.D.; Han, Z.; Li, Y.G.; Chen, G.Q. Exploring the Impact of Multitemporal DEM Data on the Susceptibility Mapping of Landslides. *Appl. Sci.* **2020**, *10*, 2518. [CrossRef]
11. Conoscenti, C.; Di Maggio, C.; Rotigliano, E. Soil erosion susceptibility assessment and validation using a geostatistical multivariate approach: A test in Southern Sicily. *Nat. Hazards.* **2008**, *46*, 287–305. [CrossRef]
12. Han, Z.; Ma, Y.F.; Li, Y.G.; Zhang, H.; Chen, N.S.; Hu, G.S.; Chen, G.Q. Hydrodynamic and topography based cellular automaton model for simulating debris flow run-out extent and entrainment behavior. *Water Res.* **2021**, *193*, 116872. [CrossRef]
13. Amorim, D.S.; Santos, C.M.D. Flies, endemicity, and the Atlantic Forest: A biogeographical study using topographic units of analysis. *Aust. Syst. Bot.* **2017**, *30*, 439–469. [CrossRef]
14. Hassani, H.; Ghazanfari, M. Landslide susceptibility zonation of the Qazvin-Rasht-Anzali railway track, North Iran. In Proceedings of the 10th International Symposium on Landslides and Engineered Slopes, Xi'an, China, 30 June–30 July 2008; p. 1911.
15. Neelakantan, R.; Yuvaraj, S. Relative effect-based landslide hazard zonation mapping in parts of Nilgiris, Tamil Nadu, South India. *Arab. J. Geosci.* **2012**, *6*, 4207–4213. [CrossRef]
16. Mergili, M.; Marchesini, I.; Alvioli, M.; Rossi, M.; Santangelo, M.; Cardinali, M.; Ardizzone, F.; Fiorucci, F.; Schneider-Muntau, B.; Fellin, W.; et al. GIS-Based Deterministic Analysis of Deep-Seated Slope Stability in a Complex Geological Setting. In *Engineering Geology for Society and Territory*; Springer: Berlin/Heidelberg, Germany, 2015; Volume 2, pp. 1437–1440.
17. Cardinali, M.; Reichenbach, P.; Guzzetti, F.; Ardizzone, F.; Antonini, G.; Galli, M.; Cacciano, M.; Castellani, M.; Salvati, P. A geomorphological approach to the estimation of landslide hazards and risks in Umbria, Central Italy. *Nat. Hazards Earth Syst. Sci.* **2002**, *2*, 57–72. [CrossRef]
18. Guzzetti, F.; Reichenbach, P.; Cardinali, M.; Galli, M.; Ardizzone, F. Probabilistic landslide hazard assessment at the basin scale. *Geomorphology* **2005**, *72*, 272–299. [CrossRef]
19. Rossi, M.; Guzzetti, F.; Reichenbach, P.; Mondini, A.C.; Peruccacci, S. Optimal landslide susceptibility zonation based on multiple forecasts. *Geomorphology* **2010**, *114*, 129–142. [CrossRef]
20. Alvioli, M.; Marchesini, I.; Reichenbach, P.; Rossi, M.; Ardizzone, F.; Fiorucci, F.; Guzzetti, F. Automatic delineation of geomorphological slope units with r.slopeunits v1.0 and their optimization for landslide susceptibility modeling. *Geosci. Model Dev.* **2016**, *9*, 3975–3991. [CrossRef]
21. Shafique, M.; van der Meijde, M.; Khan, M.A. A review of the 2005 Kashmir earthquake-induced landslides; from a remote sensing prospective. *J. Asian Earth Sci.* **2016**, *118*, 68–80. [CrossRef]
22. Zhou, G.; Esaki, T.; Qiu, C.; Sasaki, Y. A GIS-based approach of identifying slope unit from natural terrain for slope stability evaluation. *Soil Found.* **2004**, *52*, 26–28.
23. Jia, N.; Mitani, Y.; Xie, M.; Djamaluddin, I. Shallow landslide hazard assessment using a three-dimensional deterministic model in a mountainous area. *Comput. Geotech.* **2012**, *45*, 1–10. [CrossRef]
24. Romstad, B.; Etzelmüller, B. Mean-curvature watersheds: A simple method for segmentation of a digital elevation model into terrain units. *Geomorphology* **2012**, *139–140*, 293–302. [CrossRef]
25. Yan, G.; Liang, S.; Zhao, H. An Approach to Improving Slope Unit Division Using GIS Technique. *Sci. Geogr. Sinica.* **2017**, *37*, 1764–1770. [CrossRef]

26. Li, Y.G.; Chen, G.Q.; Wang, B.; Zheng, L.; Zhang, Y.B.; Tang, C. A new approach of combining aerial photography with satellite imagery for landslide detection. *Nat. Hazards* **2013**, *66*, 649–669. [CrossRef]
27. Drăguţ, L.; Blaschke, T. Automated classification of landform elements using object-based image analysis. *Geomorphology* **2006**, *81*, 330–344. [CrossRef]
28. Aplin, P.; Smith, G.M. Introduction to object-based landscape analysis. *Int. J. Geogr. Inf. Sci.* **2011**, *25*, 869–875. [CrossRef]
29. Etzelmueller, B.; Romstad, B.; Fjellanger, J. Automatic regional classification of topography in Norway. *Nor. J. Geol.* **2007**, *87*, 167–180.
30. Ermini, L.; Catani, F.; Casagli, N. Artificial Neural Networks applied to landslide susceptibility assessment. *Geomorphology* **2005**, *66*, 327–343. [CrossRef]
31. Lassueur, T.; Joost, S.; Randin, C.F. Very high resolution digital elevation models: Do they improve models of plant species distribution? *Ecol. Model.* **2006**, *198*, 139–153. [CrossRef]
32. Smith, M.P.; Zhu, A.X.; Burt, J.E.; Stiles, C. The effects of DEM resolution and neighborhood size on digital soil survey. *Geoderma* **2006**, *137*, 58–69. [CrossRef]
33. Wells, A.F.; Frost, G.V.; Macander, M.J.; Jorgenson, M.T.; Roth, J.E.; Davis, W.A.; Pullman, E.R. Integrated terrain unit mapping on the Beaufort Coastal Plain, North Slope, Alaska, USA. *Landsc. Ecol.* **2020**, *36*, 549–579. [CrossRef]
34. Chen, N.; Wang, Q. Selection of DEM Resolutions Based on the Information Amount of Terrain Factors—A Case Study of Loess Plateau Area. *J. Wuhan Univ. Inf. Sci. Ed.* **2009**, *34*, 692–695.
35. Jedlička, K. Accuracy of Surface Models Acquired from Different Sources-Important Information for Geomorphological Research. *Geomorphol. Slovaca Et Bohem.* **2009**, *9*, 17–28.
36. Papastergios, G.; Fernandez-Turiel, J.-L.; Filippidis, A.; Gimeno, D. Determination of geochemical background for environmental studies of soils via the use of HNO3 extraction and Q-Q plots. *Environ. Earth Sci.* **2010**, *64*, 743–751. [CrossRef]
37. Drăguţ, L.; Tiede, D.; Levick, S.R. ESP: A tool to estimate scale parameter for multiresolution image segmentation of remotely sensed data. *Int. J. Geogr. Inf. Sci.* **2010**, *24*, 859–871. [CrossRef]
38. Kong, C. Classification and Extraction of Urban Land-Use Information from High-Resolution Image Based on Object Multi-features. *J. China Univ. Geosci.* **2006**, *17*, 151–157. [CrossRef]
39. Han, Z.; Su, B.; Li, Y.G.; Ma, Y.F.; Wang, W.D.; Chen, G.Q. An enhanced image binarization method incorporating with Monte-Carlo simulation. *J. Cent. South Univ.* **2019**, *26*, 1661–1671. [CrossRef]
40. Han, Z.; Li, Y.G.; Du, Y.F.; Wang, W.D.; Chen, G.Q. Noncontact detection of earthquake-induced landslides by an enhanced image binarization method incorporating with Monte-Carlo simulation. *Geomat. Nat. Hazards Risk* **2019**, *10*, 219–241. [CrossRef]
41. Zhu, H.; Cai, L.; Liu, H.; Huang, W. Information Extraction of High Resolution Remote Sensing Images Based on the Calculation of Optimal Segmentation Parameters. *PLoS ONE* **2016**, *11*, e0158585. [CrossRef]
42. Woodcock, C.E.; Strahler, A.H. The factor of scale in remote sensing. *Remote Sens. Environ.* **1987**, *21*, 311–332. [CrossRef]
43. Alexandridis, T.K.; Sotiropoulou, A.M.; Bilas, G.; Karapetsas, N.; Silleos, N.G. The Effects of Seasonality in Estimating the C-Factor of Soil Erosion Studies. *Land Degrad. Dev.* **2015**, *26*, 596–603. [CrossRef]
44. Kim, M.; Madden, M.; Warner, T. Estimation of optimal image object size for the segmentation of forest stands with multispectral IKONOS imagery. In *Object-Based Image Analysis*; Springer: Berlin/Heidelberg, Germany, 2008; pp. 291–307.
45. Drăguţ, L.; Eisank, C. Object representations at multiple scales from digital elevation models. *Geomorphology* **2011**, *129*, 183–1891. [CrossRef]
46. Drăgut, L.; Eisank, C.; Strasser, T. Local variance for multi-scale analysis in geomorphometry. *Geomorphology* **2011**, *130*, 162–172. [CrossRef]
47. Benz, U.C.; Hofmann, P.; Willhauck, G.; Lingenfelder, I.; Heynen, M. Multi-resolution, object-oriented fuzzy analysis of remote sensing data for GIS-ready information. *ISPRS J. Photogramm. Remote Sens.* **2004**, *58*, 239–258. [CrossRef]
48. Duan, G.; Gong, H.; Li, X.; Chen, B. Shadow extraction based on characteristic components and object-oriented method for high-resolution images. *J. Remote Sens.* **2014**, *18*, 760–770.
49. Johnson, B.; Xie, Z. Unsupervised image segmentation evaluation and refinement using a multi-scale approach. *ISPRS J. Photogramm. Remote Sens.* **2011**, *66*, 473–483. [CrossRef]
50. Myint, S.W.; Gober, P.; Brazel, A.; Grossman-Clarke, S.; Weng, Q. Per-pixel vs. object-based classification of urban land cover extraction using high spatial resolution imagery. *Remote Sens. Environ.* **2011**, *115*, 1145–1161. [CrossRef]
51. Espindola, G.M.; Camara, G.; Reis, I.A.; Bins, L.S.; Monteiro, A.M. Parameter selection for region-growing image segmentation algorithms using spatial autocorrelation. *Int. J. Remote Sens.* **2007**, *27*, 3035–3040. [CrossRef]
52. Dongping, M.; Tianyu, C.; Hongyue, C.; Longxiang, L.; Cheng, Q.; Jinyang, D. Semivariogram-Based Spatial Bandwidth Selection for Remote Sensing Image Segmentation With Mean-Shift Algorithm. *IEEE Geosci. Remote Sens. Lett.* **2012**, *9*, 813–817. [CrossRef]
53. Tong, H.; Maxwell, T.; Zhang, Y.; Dey, V. A Supervised and Fuzzy-based Approach to Determine Optimal Multi-resolution Image Segmentation Parameters. *Photogramm. Eng. Remote Sens.* **2012**, *78*, 1029–1044. [CrossRef]
54. Schlögel, R.; Marchesini, I.; Alvioli, M.; Reichenbach, P.; Rossi, M.; Malet, J.P. Optimizing landslide susceptibility zonation: Effects of DEM spatial resolution and slope unit delineation on logistic regression models. *Geomorphology* **2018**, *301*, 10–20. [CrossRef]
55. Tian, Y.; XiaO, C.; Liu, Y.; Wu, L. Effects of raster resolution on landslide susceptibility mapping: A case study of Shenzhen. *Sci. China Ser. E Technol. Sci.* **2009**, *51*, 188–198. [CrossRef]

56. Claessens, L.; Heuvelink, G.B.M.; Schoorl, J.M.; Veldkamp, A. DEM resolution effects on shallow landslide hazard and soil redistribution modelling. *Earth Surf. Process. Landf.* **2005**, *30*, 461–477. [CrossRef]
57. Penna, D.; Borga, M.; Aronica, G.T.; Brigandì, G.; Tarolli, P. The influence of grid resolution on the prediction of natural and road-related shallow landslides. *Hydrol. Earth Syst. Sci.* **2014**, *18*, 2127–2139. [CrossRef]